Michigan State University

National Superconducting Cyclotron Laboratory

RELATIVISTIC TRANSPORT THEORY AND PION PRODUCTION IN HEAVY ION COLLISIONS

Invited talk presented at the Workshop on Relativistic Aspects of Nuclear Physics, Rio de Janeiro, 28-30 August 1991, to be published by World Scientific

WOLFGANG BAUER and BAO-AN LI

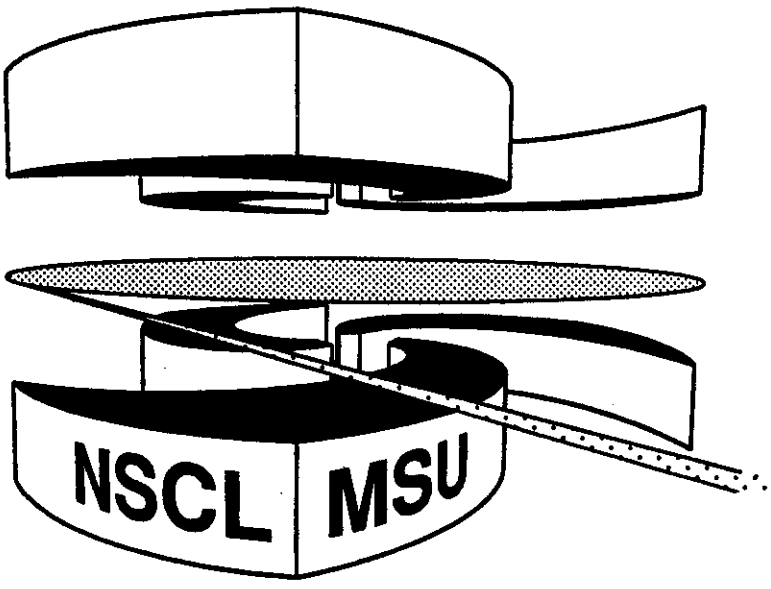

MSUCL-793 **SEPTEMBER 1991**

MSUCL-793
September, 1991

RELATIVISTIC TRANSPORT THEORY AND PION PRODUCTION IN HEAVY ION COLLISIONS†

WOLFGANG BAUER and BAO-AN LI
National Superconducting Cyclotron Laboratory
and Department of Physics and Astronomy
Michigan State University, East Lansing, MI 48824-1321, USA

ABSTRACT

We present a new transport theory for the study of hadronic matter in heavy ion collisions up to beam energies of ≈ 1 GeV/nucleon. This is done by solving coupled transport equations for nucleons, delta resonances, and pions. In this paper, we present results on pion production, such as the 'two temperature' energy spectra, preferential emission of pions in asymmetric collisions, and total pion excitation functions as obtained with our theory, and we compare them to experimental data.

1. INTRODUCTION

Relativistic ($E_{\text{beam}} \approx 1$ A·GeV) heavy ion collisions have been the subject of numerous investigations during the last decade. The observables investigated include produced pions, kaons, dilepton pairs, photons, and anti-protons, as well as emitted nucleons and light and heavy fragments.[1)] The goal in these experiments is to study nuclear matter under extreme conditions of high density and temperature, i.e. to learn more about the nuclear equation of state.[2)]

From a theoretical standpoint, this energy region provides interesting challenges. Since the beam energy is comparable to the mass of the nucleon, non-relativistic approximations to the nuclear dynamics problem are no longer suitable. In addition, the energies are high enough to create baryonic excitations, and mesonic degrees of freedom become important as well. However, the achieved energy density is well below what is required to dissolve nuclear matter into a plasma of quarks and gluons.

In order to compare to experimental observables and to study heavy ion reaction dynamics at relativistic energies one has to develop a transport theory based on quantum hadron dynamics,[3)] where the relevant degrees of freedom are nucleons, isobar excitations, and mesons. Recently, we have put forward[4)] such a transport theory. It enables us to construct a detailed theoretical model of the evolution of the phase space distribution functions for nucleons, delta resonances, and pions during the course of relativistic heavy ion reactions.

Our theory and its solution method are extensions of the Boltzmann-Uehling-Uhlenbeck model (BUU)[5)–12)] and the quantum correlation dynamics.[13)–15)] These

†Invited talk presented at the Workshop on Relativistic Aspects of Nuclear Physics, Rio de Janeiro, 28-30 August 1991, to be published by World Scientific

theories as well as ours include the effects of one-body (mean field) and two-body (nucleon-nucleon collisions) on the dynamics of the phase space distribution function. A complementary approach is that of the intra-nuclear-cascade (INC)[16)-20)] model, which treats nucleons, pions, and delta resonances as essentially free particles interacting with each other with their free scattering cross sections.

Other derivations of relativistic transport equations for heavy ion collisions and extensions of non-relativistic heavy ion transport theories have also been put forward.[21)-34)]

In this paper, we will first briefly introduce the main concepts of our theory and sketch the derivation of our coupled transport equations for pions, delta resonances, and nucleons. Then we will address the total pion production cross section and compare to the experimentally found pion excitation function. In section 4, we will present our results on the 'two temperature' shape of the pion kinetic energy spectra. Section 5 is on the observed preferential emission of pions in asymmetric systems, and in section 6 we will summarize our findings and point to future perspectives for pion physics in relativistic heavy ion collisions.

2. Hadronic Transport Theory

In relativistic heavy ion collisions at $E_{\rm beam} \approx 1$ A·GeV, the main inelastic excitation of the nucleon is the Δ (1236) resonance. All higher resonances (N^*, ...) have such low production cross sections that they have practically no influence on the nuclear dynamics. Of the mesons, we need to include the π, σ, and ω for a quantum-hadro-dynamical description of heavy ion collisions. When electromagnetic reaction probes are concerned, we also should include the ρ meson in our description.

Our starting point is a model Lagrangian similar to the one originally proposed by Walecka,[3)] but involving in addition to the nucleon fields $N(x)$ also the field of the Δ-resonance, $\Delta^\nu(x)$. Of the meson fields we not only include the $\sigma(x)$ and $\omega^\mu(x)$, but also the $\boldsymbol{\pi}(x)$. Here we have used x to denote the Minkowski four-vector $(t, \boldsymbol{r})$. The nucleon field $N(x)$ is an iso-spinor, the Δ field is described by the Rarita-Schwinger[35)] formalism as a four-vector with each component as an iso-spinor. The pion field $\boldsymbol{\pi}(x)$ is an iso-vector and a Minkowski pseudo-scalar. Furthermore, the sigma field $\sigma(x)$ is a scalar in both Minkowski and isospin space, whereas the omega field $\omega_\mu(x)$ is a Minkowski vector and an iso-scalar.

For the interactions between these fields we use the minimal coupling scheme commonly utilized for relativistic hadronic systems,

$$\mathcal{L}(x) = \mathcal{L}^0(x) + \mathcal{L}^{\rm int}(x) \; , \tag{1}$$

where $\mathcal{L}^0$ and $\mathcal{L}^{\rm int}$ are the free-field and interaction Lagrangian densities, respectively. The free Lagrangian density is

$$\mathcal{L}^0(x) \;=\; \overline{N}(x)(i\gamma^\mu\partial_\mu - m_N)N(x) + \overline{\Delta}_\nu(x)(i\gamma^\mu\partial_\mu - M_\Delta)\Delta^\nu(x)$$

$$
\begin{aligned}
&+ \frac{1}{2}[\partial_\mu \boldsymbol{\pi}(x) \cdot \partial^\mu \boldsymbol{\pi}(x) - m_\pi^2 \boldsymbol{\pi}(x) \cdot \boldsymbol{\pi}(x)] \\
&+ \frac{1}{2}[\partial_\mu \sigma(x) \partial^\mu \sigma(x) - m_\sigma^2 \sigma^2(x)] \\
&- \frac{1}{4} F_{\mu\nu}(x) F^{\mu\nu}(x) + \frac{1}{2} m_\omega^2 \omega_\mu(x) \omega^\mu(x) \; , \qquad (2)
\end{aligned}
$$

and the interaction Lagrangian density is

$$
\begin{aligned}
\mathcal{L}^{\rm int}(x) &= -i g_{\pi NN} \overline{N}(x) \gamma_5 \boldsymbol{\tau} N(x) \cdot \boldsymbol{\pi}(x) + g_{\sigma NN} \overline{N}(x) N(x) \sigma(x) \\
&- g_{\omega NN} \overline{N}(x) \gamma^\mu N(x) \omega_\mu(x) \\
&+ g_{\pi N\Delta} [\overline{\Delta}_\mu(x) \boldsymbol{T} N(x) \cdot \partial^\mu \boldsymbol{\pi}(x) + \overline{N}(x) \boldsymbol{T}^\dagger \Delta^\mu(x) \cdot \partial_\mu \boldsymbol{\pi}(x)] \\
&- i g_{\pi\Delta\Delta} \overline{\Delta}_\mu(x) \gamma_5 \boldsymbol{T} \Delta^\mu(x) \cdot \boldsymbol{\pi}(x) + g_{\sigma\Delta\Delta} \overline{\Delta}_\mu(x) \Delta^\mu(x) \sigma(x) \\
&- g_{\omega\Delta\Delta} \overline{\Delta}_\mu(x) \gamma^\nu \Delta^\mu \omega_\nu(x) \; , \qquad (3)
\end{aligned}
$$

with the field tensor $F_{\mu\nu} = \partial_\mu \omega_\nu - \partial_\nu \omega_\mu$.

We obtain the equations of motion for the different hadron fields from the above Lagrangian density by means of the Euler-Lagrange equations. The main role of the meson fields in this Lagrangian density is, however, to mediate the strong interaction between the baryons. This is strictly true for the fields $\sigma(x)$ and $\omega_\mu(x)$ which have no manifestations in terms of observable physical particles. In contrast, the pion not only mediates the interaction, but can also be observed as a real particle. By integrating over the virtual meson degrees of freedom, we obtain mean-field potential terms for the baryon interactions. We treat the pion as a real particle in order to incorporate the formation and decay of delta resonances into our formalism, and to be able to propagate real pions.

The resulting equations of motion for the baryon fields are non-local in time. In order to solve the equations, we make the instantaneous meson exchange approximation

$$
G(x - x') \approx G(\boldsymbol{r} - \boldsymbol{r}', t) \delta(t - t') \qquad (4)
$$

for the Green's function of the baryons. This approximation can be shown to be numerically valid in relativistic heavy ion collisions in the beam energy range of interest here, when the sigma and omega mesons are included.[28] However, when as in our case the lighter virtual pions are exchanged as well, then the instantaneous meson approximation is not expected to work quite as well.

Our theory uses fully relativistic kinematics and starts from a relativistically covariant Lagrangian, but due to the instantaneous meson exchange approximation our final results do not include the true relativistic effect of retardation.

In the next step, we construct densities for the nucleons, deltas, and pions from the different fields. From the equations of motion for these densities, we build up a hierarchy of n-body density matrices with their coupled equations of motion similar to the well-known BBGKY hierarchy. We truncate this hierarchy

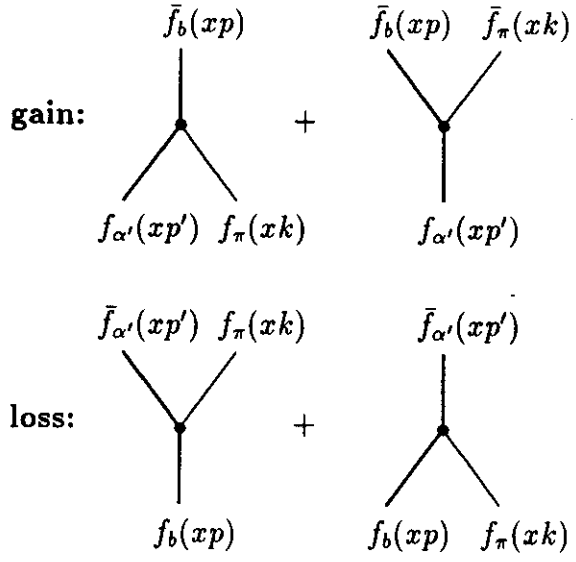

Fig. 1: Diagrammatic representation of the gain and loss terms responsible for changing the baryon phase-space distribution $f_b(x,p)$ as a result of baryon-pion collisions. The terms on the left pertain to Δ resonances, $b = \Delta$, while those on the right are for nucleons, $b = N$.

by neglecting three- and more-body correlations and obtain closed equations of motion.

In a last step, we perform Wigner transformations on the one- and two-body densities to obtain phase space distribution functions. The resulting equations of motion are given by (an explicit derivation of these results can be found in Ref. 4)

$$\frac{\partial f_b(xp)}{\partial t} + \frac{\Pi^i}{E_b^*(p)}\nabla_i^x f_b(xp) - \frac{\Pi^\mu}{E_b^*(p)}\nabla_i^x U_\mu(x)\nabla_p^i f_b(xp) + \frac{M_b^*}{E_b^*(p)}\nabla_i^x U_s \nabla_p^i f_b(xp) = I_{bb}^b(xp) + I_{b\pi}^b(xp) \tag{5}$$

for the phase space distribution functions $f_b(xp)$ of the nucleons and deltas, and

$$\frac{\partial f_\pi(xk)}{\partial t} + \frac{\boldsymbol{k}}{E_\pi}\cdot\boldsymbol{\nabla}_r f_\pi(xk) = I_{b\pi}^\pi(xk)\ , \tag{6}$$

for the phase space distribution function $f_\pi(xk)$ of the pion.

The diagrammatic representations of the collision terms $I_{bb}^b(xp)$, $I_{b\pi}^b(xp)$, and $I_{b\pi}^\pi(xk)$ are shown in Figs. 1 and 2. Their explicit forms are for baryon-baryon collisions

$$I_{bb}^b(xp) = \pi \sum_{\alpha_1\alpha_2\alpha_3, m_s^b} \iiint \frac{M_b M_{\alpha_1} M_{\alpha_2} M_{\alpha_3}}{E_b E_{\alpha_1} E_{\alpha_2} E_{\alpha_3}} W_{bb}^b(p_1\alpha_1, p_2\alpha_2, p_3\alpha_3, p\alpha_b)\cdot$$

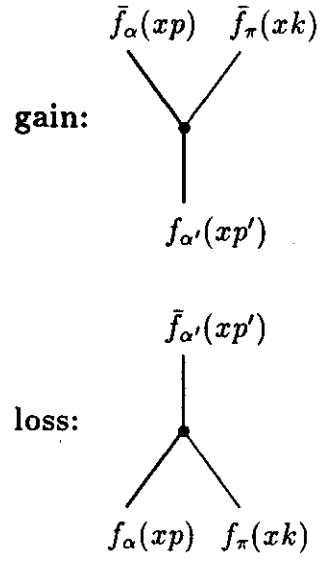

Fig. 2: Diagrammatic representation of the gain and loss terms responsible for changing the pion phase-space distribution $f_\pi(x,k)$ as a result of baryon-pion collisions.

$$[f_{\alpha_2}(xp_2)f_{\alpha_3}(xp_3)\overline{f}_{\alpha_1}(xp_1)\overline{f}_b(xp) - \overline{f}_{\alpha_2}(xp_2)\overline{f}_{\alpha_3}(xp_3)f_{\alpha_1}(xp_1)f_b(xp)]\cdot$$
$$\delta^{(4)}(p+p_1-p_2-p_3)\frac{\boldsymbol{dp}_1\boldsymbol{dp}_2\boldsymbol{dp}_3}{(2\pi)^9}\ , \tag{7}$$

and for baryon-pion interactions

$$I^b_{b\pi}(xp) = \frac{\pi}{8}\sum_{\pi\alpha' m^b_s}\iint\frac{M_bM_{\alpha'}}{E_b(p)E_{\alpha'}(p')}W^b_{b\pi}(\alpha'p',\pi k,\alpha p)\cdot \tag{8}$$
$$\{[\overline{f}_\pi(xk)f_{\alpha'}(xp')\overline{f}_b(xp) - f_\pi(xk)\overline{f}_{\alpha'}(xp')f_b(xp)]\delta^{(4)}(p'-k-p)$$
$$+[f_\pi(xk)f_{\alpha'}(xp')\overline{f}_b(xp) - \overline{f}_\pi(xk)\overline{f}_{\alpha'}(xp')f_b(xp)]\delta^{(4)}(p'+k-p)\}\frac{\boldsymbol{dp}'\boldsymbol{dk}}{(2\pi)^6}$$

and

$$I^\pi_{b\pi}(xk) = \frac{\pi}{16}\sum_{\alpha\alpha'}\iint\frac{M_\alpha M_{\alpha'}}{E_\alpha(p)E_{\alpha'}(p')}W^\pi_{b\pi}(\alpha p,\alpha'p',\pi k)\cdot \tag{9}$$
$$[\overline{f}_\pi(xk)f_{\alpha'}(xp')\overline{f}_\alpha(xp) - f_\pi(xk)f_\alpha(xp)\overline{f}_{\alpha'}(xp')]\delta^{(4)}(p'-p-k)\frac{\boldsymbol{dp}\boldsymbol{dp}'}{(2\pi)^6}.$$

Here the factors $\overline{f}_b(xp)$ are due to the Fermi-Dirac statistics of the baryons and are the manifestation of the Pauli exclusion principle

$$\overline{f}_b(xp) = 1 - f_b(xp)\ . \tag{10}$$

In the same way, the factors $\overline{f}_\pi(xk)$ are consequences of the Bose-Einstein statistics of the pions

$$\overline{f}_\pi(xk) = 1 + f_\pi(xk) \; . \tag{11}$$

Entering into the transport equations are W^b_{bb}, $W^b_{b\pi}$, and $W^\pi_{b\pi}$, the squares of the transition matrix elements for the corresponding elementary processes. They can be given in terms of the baryon-meson and baryon-baryon coupling constants.[4] But here, we take a simpler approach and replace the transition matrix elements in first Born approximation. This way, we are able to use the free, experimentally measured, widths of the resonances and cross sections in our numerical calculations.

The resulting equations are solved by using the usual test particle simulation techniques. The mean field part of the problem is solved via the particle-in-cell approach. The collision integrals are solved stochastically via Monte Carlo rejection methods. For this, the complete phase space occupation function is stored in a 6-dimensional lattice.

The resulting equation for the test particles are given by

$$\frac{d\boldsymbol{r}}{dt} = \frac{\boldsymbol{p}}{E}, \tag{12}$$

$$\frac{d\boldsymbol{p}}{dt} = -\boldsymbol{\nabla}_r U + \boldsymbol{D}^b_{bb}(p) + \boldsymbol{D}^b_{b\pi}(p) \tag{13}$$

for baryons and

$$\frac{d\boldsymbol{r}}{dt} = \frac{\boldsymbol{k}}{E_\pi}, \tag{14}$$

$$\frac{d\boldsymbol{k}}{dt} = \boldsymbol{D}^\pi_{b\pi}(k) \tag{15}$$

for pions. Here $\boldsymbol{D}^b_{bb}(p)$, $\boldsymbol{D}^b_{b\pi}(p)$ are the changes of the baryon momentum distribution due to baryon-baryon collisions and baryon-pion collisions, respectively, in accordance with the collision integrals I^b_{bb} and $I^b_{b\pi}$. $\boldsymbol{D}^\pi_{b\pi}(k)$ is the corresponding change in the pion phase space distribution due to baryon-pion collisions corresponding to the collision integral $I^\pi_{b\pi}$. They are calculated in a similar manner as in the cascade models, namely by dividing the reaction time into small time steps and solving the collision integrals within each time step via a Monte Carlo simulation method.[16),17)] Further numerical details can be obtained from Ref. 36.

3. PION EXCITATION FUNCTION

The first observable that can be studied with a hadronic transport theory is the total pion multiplicity produced in heavy ion collisions. The BUU/VUU model has been found to successfully reproduce this overall feature of the pion excitation function[37)] for central La + La collisions in the beam energy region between 500 and 1300 MeV/nucleon.[38)] In the same study, it was shown[37)] that intra-nuclear-cascade

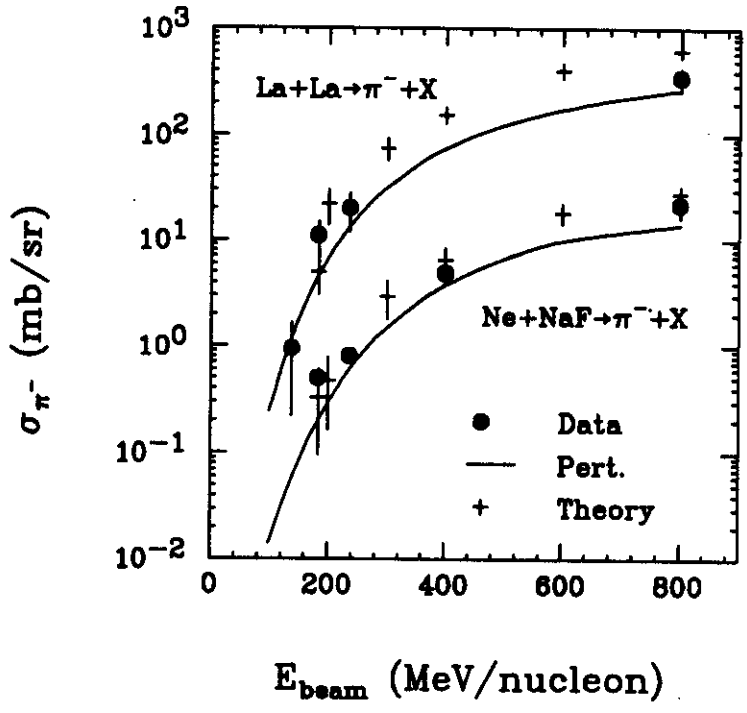

Fig. 3: Production cross section for negative pions produced at $\theta = 90°$ as a function of the beam energy for light and heavy ion systems. The filled circles represent the preliminary data,[41)-43)] the crosses are the results of our transport calculations, and the solid lines are from a perturbative approximation to the full theory.

calculations clearly overpredict the data. We should stress at this point that the magnitude of this disagreement cannot alone be explained by compressional effects due to the nuclear mean field,[19)] in contrast to earlier interpretations.[39)] At present it thus seems unlikely that we will be able to extract the value of the nuclear compressibility from absolute pion production cross sections.[40)]

Here we present a comparison of our transport calculations to the excitation functions for the production of negative pions in (near) symmetric collisions of heavy and light nuclei at various beam energies. In Fig. 3, we compare our calculations (crosses) to the preliminary data of Miller *et al.*[41)-43)] (filled circles). They have compiled pion excitation function for beam energies down below the threshold value of $E_{\rm thr.} = 2M_\pi + M_\pi^2/2M_N \approx 290$ MeV. The goal in their investigation is to see to what degree collective production of pions can be observed.

As can be observed from Fig. 3, the agreement between theory and experiment is quite good for both systems and for all beam energies. However, as one approaches the threshold region the theoretical statistical error bars become prohibitively large. We therefore also show (solid lines) the results of a perturbative approximation to the theory. In this approximation we compute the production probability for pions in every individual nucleon-nucleon collision. Instead of using a Monte Carlo

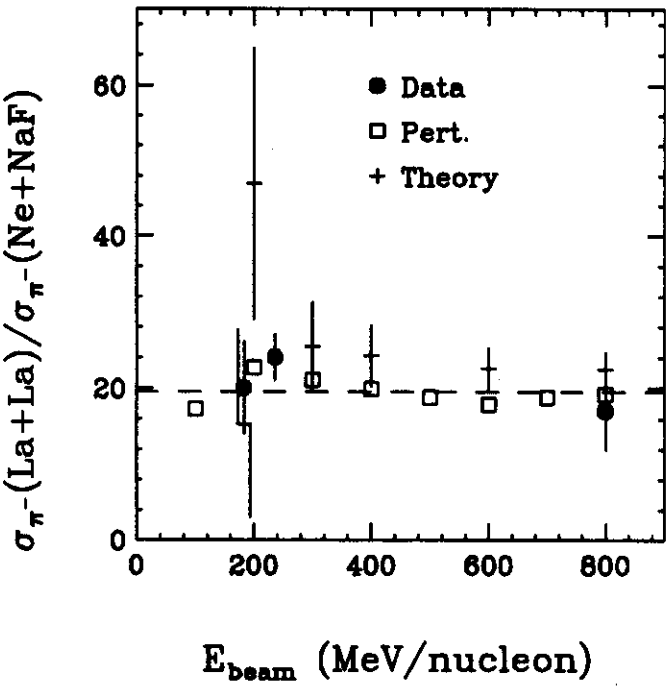

Fig. 4: Ratio of the negative pion production cross section at 90° for heavy (La+La) and light (Ne+NaF) systems. Crosses: Theory, squares: perturbative approximation to the full theory, filled circles: preliminary data from Ref. 42. The dashed line is the average over all beam energies for the perturbative calculations.

procedure to decide if the pion will actually be produced, and then propagating it, we simply add up all elementary probabilities for pion production to obtain the total production cross section

$$\sigma_\pi = \int db^2 \sum_{\mathrm{coll}(b)} \int \frac{d\Omega^{if}}{4\pi} \mathcal{L} P_\pi(p_1,p_2) \overline{f}_b(x,p_3) \overline{f}_b(x,p_4) \overline{f}_\pi(x,k) \chi_{\mathrm{abs}}(A). \qquad (16)$$

Here, $P_\pi = \sigma_\pi/\sigma_{\mathrm{tot}}$ is the pion production probability for two nucleons having 4-momenta p_1 and p_2, and it is parametrized using experimental free nucleon-nucleon cross sections.[44),45)] $\mathcal{L}$ represents a Lorentz transformation from the nucleon-nucleon c.m. system to the system of calculation.

The function $\chi_{\mathrm{abs}}(A)$ represents the effect of pion reabsorption,

$$\chi_{\mathrm{abs}}(A) = \exp(-R(A)/\alpha). \qquad (17)$$

For the perturbative calculations in Fig. 3, a mean pion absorption length of $\alpha = 4.5$ fm was chosen.

While we are able to follow the pion test particles and are able to calculate the pion absorption cross section from detailed balance considerations in our full calculation, we have to use this approximation in the perturbative calculations.

For light systems (C+C), we have shown[46] that it is possible to explain the total yield and also the energy spectra of neutral pions at beam energies between 60 and 84 MeV/nucleon[47),48] by this perturbative approach, which is based on the assumption that all pions are generated in individual nucleon-nucleon collision without any collective contributions. Other calculations have resulted in the same conclusion.[49)-52]

At high beam energies (> 400 MeV/nucleon), there is also very little doubt that an individual nucleon-nucleon collisions production picture is right. However, for heavy systems and low beam energies there is still debate as to what degree collective production of pions may be involved.[53] This is because collective production models[54)-57] predict a total production probability for a particle proportional to the square of the 'charge', in this case the baryon number. In contrast, the individual nucleon-nucleon collisions production models predict only a linear dependence on this 'charge'. There are other scaling factors which obscure this simple scaling picture ($\sigma_\pi \propto A^2$ vs. $\sigma_\pi \propto A$), primarily due to reabsorption of the pions. However, by taking the ratio of production cross sections for pions from heavy and from light systems, one should be able to obtain hints on the degree of collectivity involved. A change in this ratio as the beam energy approaches the threshold energy for individual $N + N \rightarrow N + N + \pi$ processes should signal the presence of collective behavior.

In Fig. 4, we present such a compilation. As can be seen, the preliminary data[42] (full circles) show no such enhancement, even for a beam energy of 183 MeV/nucleon. The full theoretical calculations (crosses) show almost exactly the same ratio as the experiments. The discrepancy at 200 MeV/nucleon is statistically not significant. The perturbative calculations (squares) do not have the problems of low statistics, and we can clearly see that the ratio extracted from this approximation has no sizable deviations from its mean value of 19.5 (dashed line). Our preliminary conclusion from this study is that there are no hints of collective contributions to subthreshold pion production in heavy ion systems as of this date.

4. CRITICAL PION OPACITY

We propose a new effect, which should be visible by careful examination of the pion excitation function as a function of beam energy, and which we have named 'critical pion opacity'.[58] This effect should manifest itself as an increase in pion absorption in nuclear matter close to the nuclear matter 'liquid-gas' critical point.

We expect nuclear matter to have a phase diagram similar to a Van der Waals gas, because the nuclear interaction exhibits short range repulsion and long range attraction.[59),60] Consequently, we should expect infinite nuclear matter to be able to go through a phase transition from the liquid to the gas phase. This phase transition is expected to be of first order, terminating in a second order phase transition at the critical point. It should be stressed here that there is no firm experimental evidence for the existence of a second order phase transition and a

corresponding critical point as of yet. However, it is hoped that with the new heavy ion accelerators and new detector arrays covering almost the full solid angle this interesting point of the nuclear phase diagram will be studied in detail. In a previous publication, we have pointed out methods to look for the critical point, to treat the finite size effects and to determine the critical exponents.[61] At this critical point, the density fluctuations, $\langle \rho^2 \rangle$, are at maximum, as expected from any second order phase transition.[62]

Pion absorption is sensitive to these fluctuations in the baryon density. This is due to the fact that pion absorption is a two-nucleon process (pion absorption on one nucleon is forbidden for simple kinematical reasons), predominantly via $N + \pi \rightarrow \Delta$, $\Delta + N \rightarrow N + N$. Since the Δ can decay again into $\pi + N$, the above process has to take place on short inter-nucleon distances of the order[63]

$$d = \frac{\hbar}{\sqrt{M_N M_\pi}} \approx 0.5 \text{ fm}. \tag{18}$$

Thus the pion absorption cross section exhibits a dependence of $\sigma_{abs} \propto \rho^2$.

Our proposed scenario is now as follows: Pions are produced in the initial high density phase of the nuclear reaction ($\rho_0 < \rho < 2\rho_0$) at a beam energy of $E_{\text{cm}} \approx 20 - 30$ MeV/A. As the system expands and cools, some initial condition for E_{cm} will result in the nuclear system passing through the critical point of the fragmentation phase transition. Pions which were generated with low enough kinetic energies will still be in the nuclear system and will then be absorbed at an increased rate due to the density fluctuations around the critical point, whereas the high energy pions will have left the system before the development of the critical fluctuations. We therefore propose to study the ratio

$$\mathcal{R}_\pi(E_{\text{beam}}) = \frac{\sigma_\pi(E_\pi < E^\pi_{\text{cr}})}{\sigma_\pi(E_\pi > E^\pi_{\text{cr}})}, \tag{19}$$

where E_π is the pion kinetic energy in the c.m. frame, and E^π_{cr} is the maximum kinetic energy a pion can have and still remain in the nuclear system when the phase transition occurs. We estimate this energy to be $E^\pi_{\text{cr}} \approx 30 - 70$ MeV, depending on the initial compression and total mass of the nuclear system. Our prediction is that the ratio $\mathcal{R}$ has a local minimum at the beam energy corresponding to an evolution of the nuclear system passing through the critical point of the nuclear matter liquid-gas phase transition.

The above scenario can of course not be studied in the framework of our transport model, because our model is based on a truncation of the many-body hierarchy on the three-body level and is therefore not suited to study physics at the critical point of a second order phase transition.

It should be pointed out that our proposed effect has no connection to the proposed pion condensation,[64),65),66] an admixture of pion-like modes to the ground state of dense hadronic matter at high densities. It was proposed that this collective instability in nuclear matter should lead to critical scattering phenomena

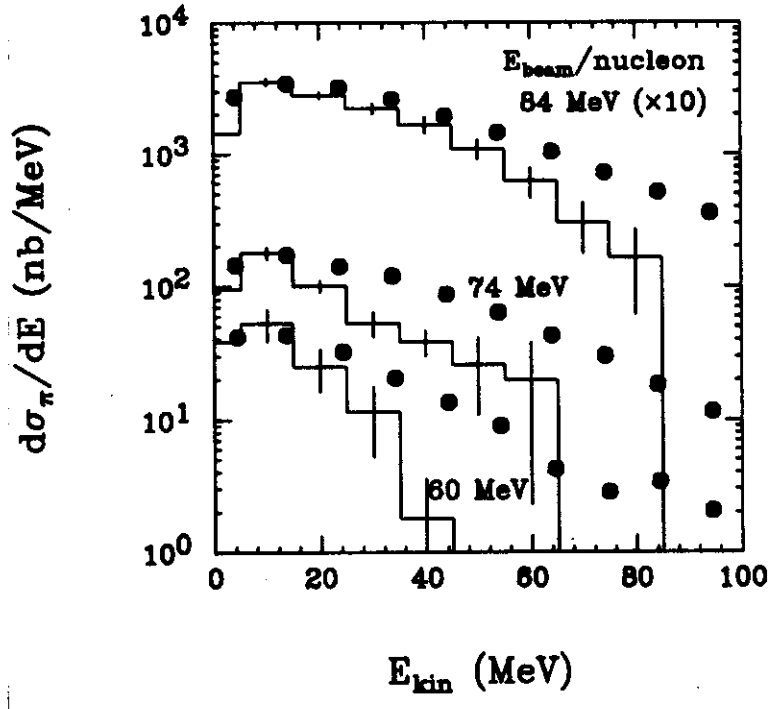

Fig. 5: Pion kinetic energy spectra from the reaction $^{12}C + {}^{12}C \rightarrow \pi^0 + X$ for three different beam energies. The data (filled circles) are from Ref. 47, and the histograms represent the calculations using the perturbative model introduced in section 3.[46)]

associated with a reduced nuclear transparency[67)] and to an increase in threshold pion production due to the increased nuclear stopping power in association with this effect.[54)] Whether this pion condensed state can exist in nature, however, is still an open question,[68)] and so far no conclusive positive experimental results regarding pion condensation have been reported.

5. PION SPECTRA

In this section, we will present our results on the calculation of kinetic energy spectra for pions produced in heavy ion collisions. In an earlier study[46)] we had used the perturbative model introduced in section 3 to predict pion kinetic energy spectra from subthreshold reactions at $E_{\rm beam}$ = 60, 74, 84 MeV/nucleon. The comparison of the experimental data of Noll *et al.*[47)] (filled plot symbols) and our calculations (histograms with statistical error bars) is shown in figure 5. We showed that without the inclusion of the Δ degree of freedom it is not possible to reproduce the experimentally measured pion kinetic energy spectra.

For the 84 MeV/A beam energy, there is reasonable agreement between data and perturbative calculations. However, we can see that for the lower beam energies

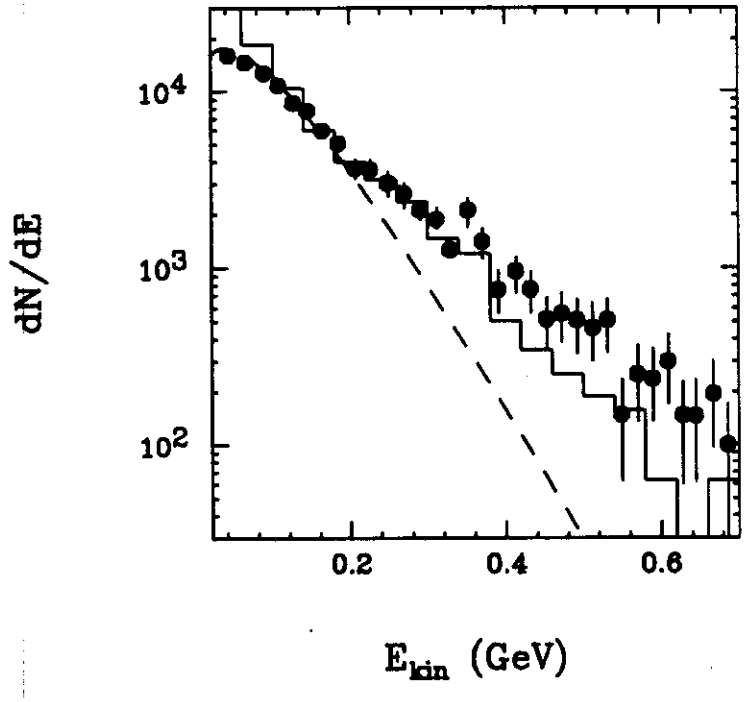

Fig. 6: Comparison between our calculations (histogram) and the experimental data[72] for central La + La collisions at E/A = 1.35 GeV (filled circles with error bars). The dashed line represents a single-temperature fit to the low-energy part of the experimental pion spectrum with $T = 58$ MeV.

the agreement becomes worse. It is found that the experimental pion spectra follow

$$\frac{1}{p_\pi E_\pi}\frac{d\sigma_\pi}{dE_\pi} \propto \exp\left(-\frac{E_\pi}{T(E_{\rm beam})}\right) \tag{20}$$

with the inverse slope parameters $T(E_{\rm beam})$ saturating at a lower value of about 15 MeV as the beam energy approaches 0.[69] This effect cannot be explained by our simple perturbative model. Niita[70] claims that it is due to the contribution of the high momentum components above the Fermi level of the nuclear wave function, which are not included in this semiclassical approach, but which can be included in an empirical fashion.

At higher beam energies around 1 GeV per nucleon, the average produced pion multiplicity is high enough for us to calculate pion kinetic energy spectra with the aid of the full transport model introduced in section 2.

In this beam energy region, the experimentally observed pion energy spectra from central heavy ion collisions show a concave shape. This phenomenon has been observed in Ar + KCl collisions at $E_{\rm beam} = 1.8$ AGeV,[71] La + La at 1.35 AGeV,[72] and Au + Au at 1.15 AGeV.[73] Empirically, the data can be fit with a

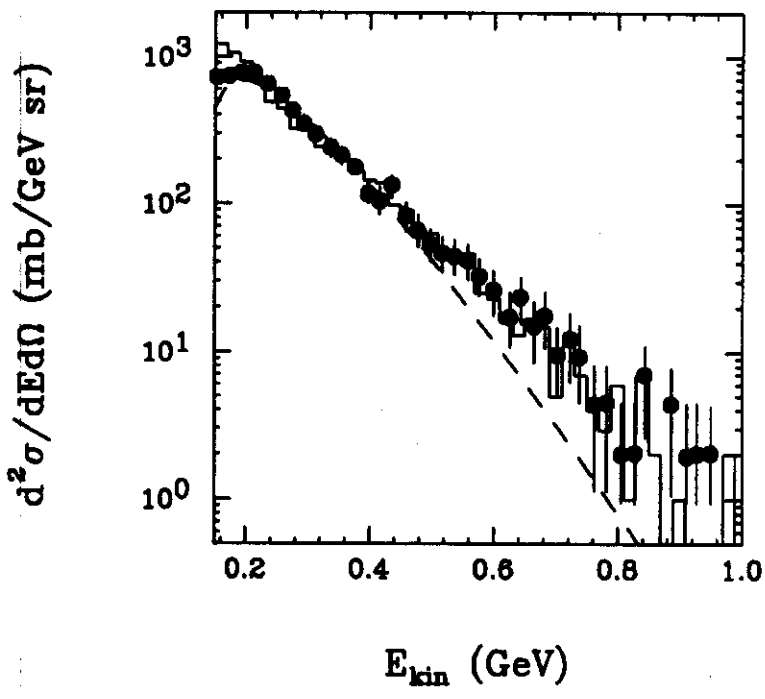

Fig. 7: Comparison between our calculations (histogram) and the experimental data[71] for central Ar+KCl collisions at E/A = 1.8 GeV (filled circles with error bars). The dashed line represents a single-temperature fit to the low-energy part of the experimental pion spectrum with $T = 63$ MeV.

two temperature fit

$$\frac{1}{p_\pi E_\pi}\frac{d\sigma\pi}{dE_\pi} = \alpha_1 \exp\left(-\frac{E_\pi}{T_1}\right) + \alpha_2 \exp\left(-\frac{E_\pi}{T_2}\right) \tag{21}$$

For example,[72] a one-temperature fit with $T = 58$ MeV to the La + La data yields a χ^2 per degree of freedom of 3.4, whereas a two-temperature fit ($T_1 = 45$ MeV and $T_2 = 101$ MeV) to the same data has a χ^2 per degree of freedom of 0.9.

Proposed possible explanations for this effect include the collective flow of intermediate deltas, a changed pion dispersion relation in medium, the population of the N^* resonance, and direct pions from a Dalitz decay

$$N + N \rightarrow N + N + \pi \tag{22}$$

without intermediate resonance formation.[71)-74)]

Using the framework of our transport model of section 2, we performed calculations of the energy spectra for the above systems. In figures 6 and 7, we compare the results of theses calculations to the data. First, we note that the magnitude and shape of the experimental and theoretical pion spectra are in very good agreement. The dashed lines in both figures represent the best one-temperature fits to

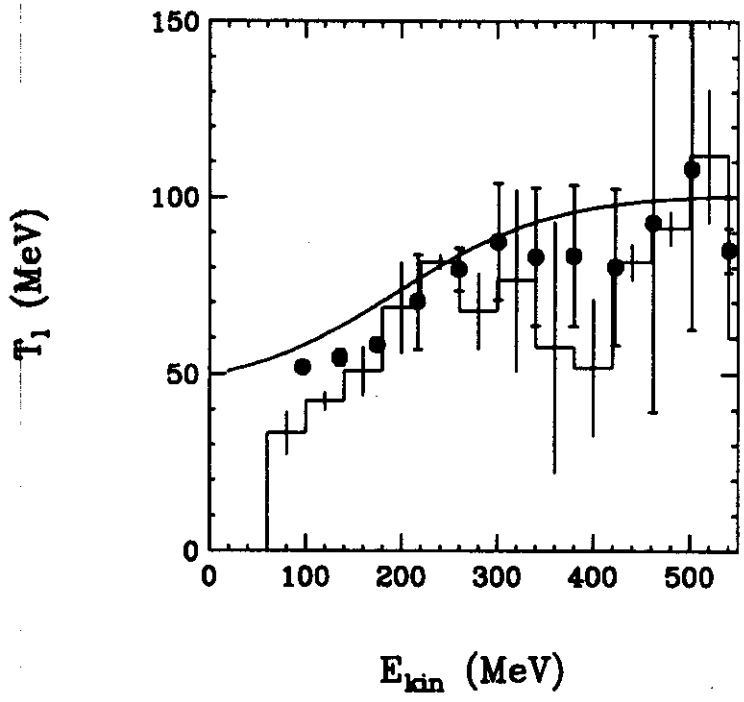

Fig. 8: Local slope T_l as a function of the pion kinetic energy for the central heavy ion reaction La + La at $E_{beam}/A = 1.35$ GeV. Histogram: Transport calculations; Filled circles: Data as extracted from Ref. 72. The solid line represents T_l as extracted with equation 23 from a two-temperature fit, Eq. 21, with $T_1 = 45$ MeV, $T_2 = 101$ MeV, and $\alpha_1/\alpha_2 = 5.0$, to the experimental data.

the data at low pion kinetic energies. One can clearly observe that the data as well as the calculations systematically deviate from a one-temperature shape at higher energies.

To show the change in apparent temperature as a function of the kinetic energy of the pions, we introduce a local slope[75]

$$T_l = -\left(\frac{d}{dE}\ln\left[\frac{1}{p_\pi E_\pi}\frac{d\sigma}{dE_\pi}\right]\right)^{-1} \tag{23}$$

and plot it as a function of E_π.

In figure 8 we perform such an analysis and compare our calculations (histogram) with the experimental data (filled circles). The error bars were in both cases obtained by taking forward and backward difference formulas to compute T_l and using the difference in the results as an indication for the error. It is clear that data and calculations are in good agreement (within the error bars), and that they both show a change in local slope not compatible with a one-temperature picture. In this figure, a one-temperature spectrum would show up as a straight horizontal line. For comparison, we also show the local slope extracted from the

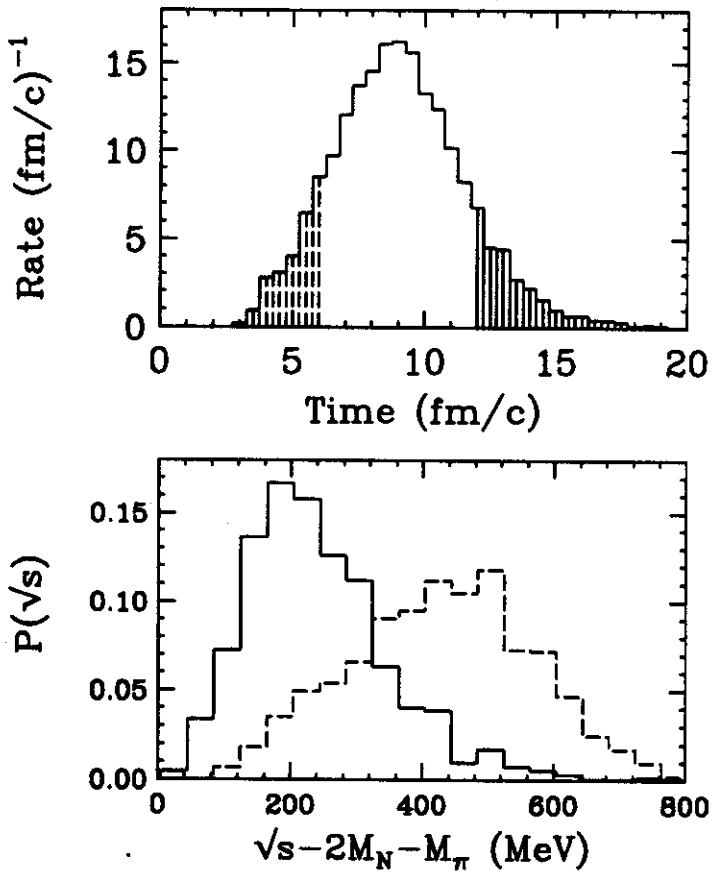

Fig. 9: Upper panel: Time evolution of the calculated production rate for delta resonances in central La+La collisions at E/A = 1.35 GeV. Lower panel: Normalized distribution of nucleon-nucleon center-of-mass energies, $\sqrt{s}$ for two different time intervals. Dashed line: $t \leq 6$ fm/c (dashed shaded regions in the upper panel); solid line: $t \geq 12$ fm/c (solid shaded region in the upper panel).

best two-temperature fit according to Eq. 21 to the data ($T_1 = 45$ MeV, $T_2 = 101$ MeV, and $\alpha_1/\alpha_2 = 5.0$).

What is now the origin of this apparent two-temperature shape of the pion kinetic energy spectra? In our calculations, we adjust the nuclear compressibility and with it the baryon flow between a stiff and a soft nuclear equation of state. We find that the effect appears independently from the choice for this parameter and conclude that collective delta flow is not causing the phenomenon. By turning on and off the production of N^*-resonances and direct pions, we are also able to exclude these two explanations.

We found two reasons for the concave shape of the pion spectra.[36),76)] They are both of a dynamical nature and are only accessible by a time-dependent transport theory, but cannot be reproduced in a thermal model.

The first source for the concavity is illustrated in figure 9. During the course

of the heavy ion reaction, the average available center-of-mass energy in nucleon-nucleon collisions decreases. In the initial stage, we have exclusively first-chance collisions between a nucleon at projectile rapidity and another one at target rapidity. In later stages, the mid-rapidity region becomes increasingly populated by nucleons due to previous collisions. These mid-rapidity nucleons can also have collisions with projectile or target rapidity nucleons, which on average have lower c.m. energy than the first chance collisions and therefore produce lower energy pions. In figure 9, this effect is clearly visible in the $\sqrt{s}$ probability distributions for the two time intervals indicated by the shading.

The second reason is the energy dependence of the pion absorption cross section. The main dynamical effect here is the fact that the high energy pions are generated early in the heavy ion reaction. At this time, the average baryon density is still very high, and since the pion absorption cross section is $\propto \rho_b^2$, the pion absorption is strong. Pions produced later have lower absorption cross sections, because the baryon density has decreased. This dynamical effect has to be convoluted with the energy dependence of the pion absorption cross section resulting from detailed balance. We thus have a different effective dynamical absorption of pions in central heavy ion collisions than in proton-proton collisions.

We should point out at this point, that we do not only have two temperatures in our calculations. Rather the concave shape of the pion kinetic energy spectrum comes from different contributions of different phases of the reaction and is a result of a gradual thermalization and approach to thermal equilibrium.

Finally, we remark that a two-temperature pion spectrum has also been observed in ultra-relativistic heavy ion collisions.[77)-79)] The origin of this soft-pion enhancement has been vigorously debated in the literature.[80)-83)] The experience from our study suggests that the concave pion spectrum observed at ultra-relativistic energies may also have a dynamical origin like the one discussed above. This explanation should be thoroughly investigated before more exotic explanations like a changed pion dispersion relation or a pion chemical potential of the the order m_π due to Bose-Einstein correlations from pion-pion collisions are studied.

6. PION 'FLOW'

The existence of a collective flow signature among the final state baryons of relativistic heavy ion collisions at beam energies around 1 GeV/nucleon has been firmly established by the in-plane transverse momentum analysis.[84)] Several groups have also tried to obtain signatures for collective flow of pions produced in these heavy ion collisions.[85),86),87)] These groups studied the average transverse momentum measured in the reaction plane, $\langle p_x \rangle$, as a function of pion rapidity, y,

$$y = \frac{1}{2} \ln \frac{E + p_{\parallel}}{E - p_{\parallel}} \,. \tag{24}$$

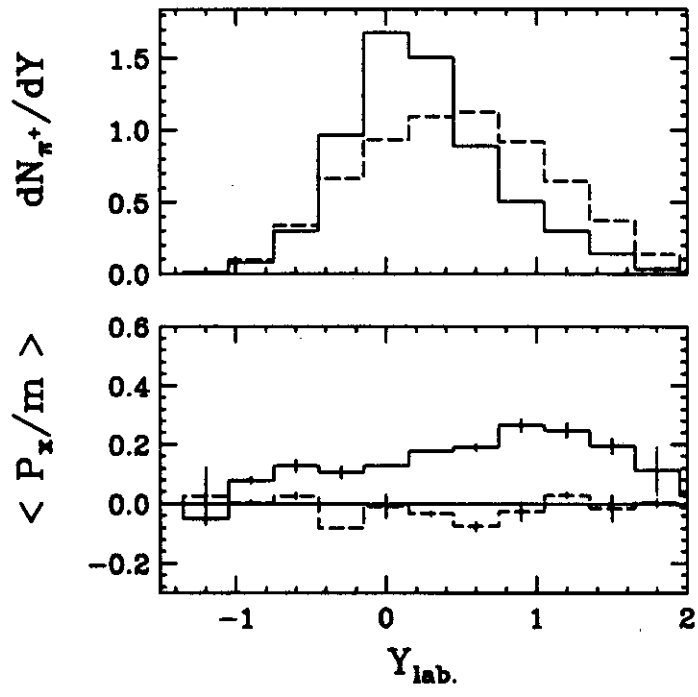

Fig. 10: Upper figure: π^+ rapidity distribution calculated with (solid histogram) and without (dashed histogram) the pion reabsorption channels for the reaction of Ne + Pb at E/A = 800 MeV and an impact parameter of 3 fm. For ease of comparison, the overall normalization of both curves was fixed to the same value. Lower figure: Calculated π^+ transverse momentum distributions in the true reaction plane with (solid histogram) and without (dashed histogram) the pion reabsorption channels.

Here, one of the most striking results from the DIOGENE collaboration[87] is that the in-plane transverse momentum of pions is always positive, even for backward rapidities, for the asymmetric systems studied (Ne or Ar) + (Nb or Pb).

Other presently available theories have so far not been able to quantitatively reproduce this effect. The Intra-Nuclear-Cascade model predicts values of $\langle p_x \rangle$ compatible with 0 over the whole rapidity range,[87], and a Quantum-Molecular Dynamics model calculation[88] indicates that the introduction of the mean field describes some of the experimental effect, but the model predicts less asymmetry than observed in experiment.

Within the framework of our model, we have conducted a theoretical study[89] of the preferential emission of pions in the heavy ion collisions described above. In our investigation we know the reaction plane *a priori*, and we refer to it as the true reaction plane. We first calculate the transverse pion momentum distribution in this plane to investigate the mechanism causing the effect.

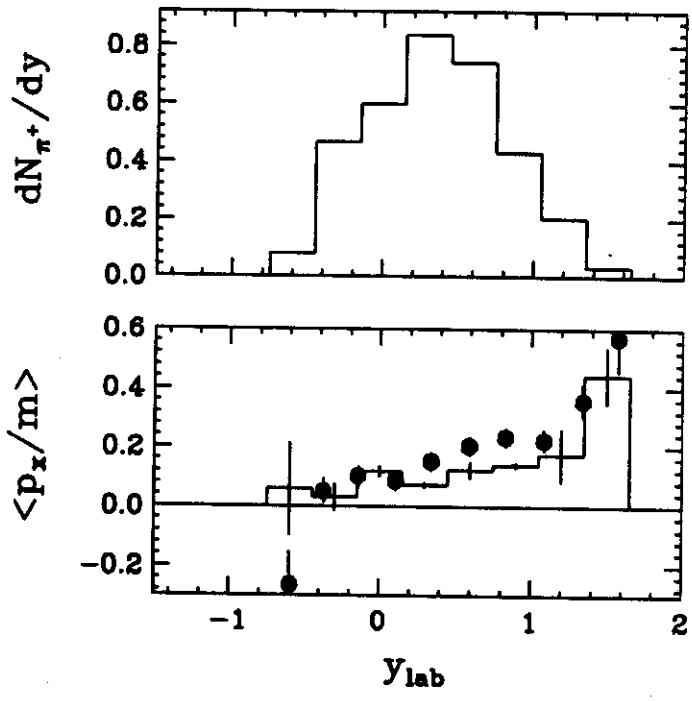

Fig. 11: Upper figure: calculated π^+ rapidity distribution after using the detector filter cut for the Ne + Pb reaction at E/A = 800 MeV. Lower figure: Comparison between the experimental pion transverse momentum distribution (filled circles) and the model calculation (histogram) for the same reaction.

In Fig. 10, we show the π^+ rapidity and scaled transverse momentum distributions in this true reaction plane for the reaction Ne + Pb at 800 MeV/nucleon. The calculations were performed at an impact parameter of 3 fm, which coincides with the average impact parameter derived from the experimental[87] trigger conditions. We can see that the rapidity distribution has its maximum near the center of mass rapidity (0.1), and that the average transverse momentum of the pions is positive for every rapidity bin.

We have investigated the question whether this effect can be caused by collective flow of intermediate Δ resonances. By varying the nuclear compressibility between a stiff and a soft nuclear equation of state, we found that the baryon flow changes in magnitude, but the pion transverse momentum distribution as a function of rapidity remained unchanged within statistical error bars. Therefore collective flow of the intermediate Δ resonances can be excluded as the origin of the phenomenon.

We propose that the observed asymmetry in the pion transverse momentum spectrum is due to a target shadowing effect in the asymmetric heavy ion system. This can be tested by switching off all pion reabsorption and Δ rescattering

channels. The result of this calculation is also displayed in figure 1 (dashed histogram). It can clearly be observed that the bulk of the pion transverse momentum asymmetry is due to a target shadowing effect. Without the absorption channels present, the pion transverse momentum spectrum becomes compatible with 0 for all rapidity intervals.

In order to compare to the experimental data of the DIOGENE collaboration, we cannot use the true reaction plane, but we have to estimate the reaction plane in the same way as done in experiment. We calculate the vector

$$\boldsymbol{Q}_j = \sum_{i \neq j} w_i \boldsymbol{p}_{\perp i} \tag{25}$$

from the momenta $\boldsymbol{p}_{\perp i}$ of the detected protons. For the detection of all particles, we have made a full simulation of the detector acceptance of the DIOGENE collaboration. In the above equation, the weights w_i are

$$w_i = y_i - \frac{1}{Z_d} \sum_{j=1}^{Z_d} y_j \tag{26}$$

where Z_d is the total number of detected protons. These weights were chosen by the experimental collaboration, because it is not *a priori* known how many target and projectile nucleons constitute the participant zone.

The transverse momentum of each pion in the estimated reaction plane is then calculated via

$$p_{xj} = \frac{\boldsymbol{Q}_j \cdot \boldsymbol{p}_{\perp j}}{|\boldsymbol{Q}_j|} \, . \tag{27}$$

In Fig. 11, we perform a comparison between the experimental data (filled circles) and our calculations. Again, the error bars in the theoretical calculations as well as those in experiment are of statistical nature. Within those error bars, our calculations are in reasonable agreement with the data.

7. SUMMARY

We have presented a new transport theory for relativistic heavy ion reactions in the beam energy region of 1 GeV/nucleon. Our theory is for hadronic matter and includes Δ and π degrees of freedom. Comparisons to different experimental data sets for total pion excitation functions, ratios of pion excitation functions, pion kinetic energy spectra, the two-temperature appearance of pion spectra, and preferential emission of pions in asymmetric heavy ion collisions indicate that our model is able to describe most features of pion production physics in relativistic heavy ion reactions properly. This supports the conclusion that the approximations entering our derivations should be approximately valid. A working transport theory for this energy region is important and will be used in the future to compare

to experimental data to be able to sort out observations which are due to 'conventional' transport processes (= processes that can be explained by our model) and new physics phenomena in relativistic heavy ion physics. The most important question to address in the future is why the more interesting medium modifications and many-body effects have so far not yielded a more significant disagreement between experiment and theory.

We acknowledge helpful discussions and collaborations with W. Benenson, G.F. Bertsch, P. Danielewicz, J. Gosset, J. Miller, J. Randrup, E.V. Shuryak, and S.J. Wang. This research was supported by the National Science Foundation under Grants PHY-8906116 and PHY-9017077 and under the Cooperative Science - Latin America program.

8. REFERENCES

1. Advances in Nuclear Dynamics – Proc. of the Workshop on Nuclear Dynamics VII, Key West, Florida, USA, January 26 - February 2, 1991, *Ed.:* Bauer, W., and Kapusta, J., (World Scientific, Singapore, 1991).
2. The Nuclear Equation of State – Proc. of the NATO Advanced Study Institute, Peñiscola, Spain, May 22 - June 3, 1989, *Ed.:* Greiner, W., and Stöcker, H., (Plenum Press, New York, 1989).
3. Serot, B.D., and Walecka, J.G., Adv. in Nucl. Phys. 16, *Ed.:* Negele, J.W., and Vogt, E., (Plenum Press, New York, 1986).
4. Wang, S.-J., Li, B.-A., Bauer, W., and Randrup, J., Ann. Phys. (N.Y.) 209, 251 (1991).
5. Bertsch, G.F., Kruse, H., and Das Gupta, S., Phys. Rev. C29, 673 (1984).
6. Kruse, H., Jacak, B.V., and Stöcker, H., Phys. Rev. Lett. 54, 289 (1985).
7. Bauer, W., Bertsch, G.F., Cassing, W., and Mosel, U., Phys. Rev. C34, 2127 (1986).
8. Stöcker, H., and Greiner, W., Phys. Rep. 137, 277 (1986).
9. Gregoire, C., Remaud, B., Sebille, F., Vinet, L., and Raffray, Y., Nucl. Phys. A465, 317 (1987).
10. Bertsch, G.F., and Das Gupta, S., Phys. Rep. 160, 189 (1988).
11. Schuck, P., Hasse, R.W., Jaenicke, J., Gregoire, C., Remaud, B., Sebille, F., and Suraud, E., Prog. Part. Nucl. Phys. 22, 181 (1989).
12. Cassing, W., and Mosel, U., Prog. Part. Nucl. Phys. 25, 235 (1990).
13. Wang, S.-J., and Cassing, W., Ann. Phys. (N.Y.) 159, 328 (1985).
14. Wang, S.-J., and Cassing, W., Nucl. Phys. A495, 371c (1989).
15. Cassing, W., and Wang, S.-J., Z. Phys. A337, 1 (1990).
16. Randrup, J., Nucl. Phys. A314, 429 (1979).
17. Cugnon, J., Mizutani, T., and Vandermeulen, J., Nucl. Phys. A352, 505 (1981).
18. Cugnon, J., Kinet, D., Vandermeulen, J., Nucl. Phys. A379, 553 (1982).
19. Kitazoe, Y., Sano, M., Toki, H., and Nagamiya, S., Phys. Lett. 166B, 35 (1986) and Phys. Rev. Lett. 58, 1508 (1987).

20. Cugnon, J., and Lemaire, M.C., Nucl. Phys. A489, 781 (1988).
21. Ko, C.M., Li, Q., and Wang, R., Phys. Rev. Lett. 59, 1084 (1987).
22. Ko, C.M., and Li, Q., Phys. Rev. C37, 2270 (1988).
23. Li, Q., and Ko, C.M., Mod. Phys. Lett. A3, 465 (1988).
24. Blättel, B., Koch, V., Cassing, W., and Mosel, U., Phys. Rev. C38, 1767 (1988).
25. Li, Q., Wu, J.Q., and Ko, C.M., Phys. Rev. C39, 849 (1989).
26. Siemens, P.J., Soyeur, M., White, G.D., Lantto, L.J., and Davies, K.T.R., Phys. Rev. C40, 2641 (1989).
27. Schönhofen, M., Cubero, M., Gering, M., Sambataro, M., Feldmeier, H., and Nörenberg, W., Nucl. Phys. A504, 875 (1989).
28. Blättel, B., Koch, V., Lang, A., Weber, K., Cassing, W., and Mosel, U., in Ref. 2, p. 321 (1989).
29. Weber, K., Blättel, B., Koch, V., Lang, A., Cassing, W., and Mosel, U., Nucl. Phys. A515, 747 (1990).
30. Cubero, M., Schönhofen, M., Friman, B.L., and Nörenberg, W., GSI preprint GSI-90-30.
31. Botermans, W., and Malfliet, R., Phys. Rep. 198, 115 (1990).
32. Wolf, Gy., Batko, G., Cassing, W., and Mosel, U., Nucl. Phys. A517, 615 (1990).
33. Wolf, Gy., Batko, G., Cassing, W., Mosel, U., Niita, K., and Schäfer, M., Proc. of Corinnes, Nantes, France, *Ed.:* Ardouin, D., (World Scientific, Singapore, 1990).
34. Davis, J.E., and Perry, R.J., Phys. Rev. C43, 1893 (1991).
35. Rarita, W., and Schwinger, J., Phys. Rev. 60, 61 (1941).
36. Li, B.-A., and Bauer, W., Phys. Rev. C44, 450 (1991).
37. Molitoris, J.J., Stöcker, H., and Winer, B.L., Phys. Rev. C36, 220 (1987).
38. Harris, J.W., Odyniec, G., Pugh, H.G., Schroeder, L.S., Tincknell, M., Rauch, W., Stock, R., Bock, R., Brockmann, R., Sandoval, A., Ströbele, H., Renfordt, R.E., Schall, D., Bangert, D., Sullivan, J.P., Wolf, K.L., Dacal, A., Guerra, C., and Ortiz, M.E., Phys. Rev. Lett. 58, 463 (1987) and Phys. Lett. 153B, 377 (1985).
39. Stock, R., Brockmann, R., Harris, J.W., Sandoval, A., Ströbele, H., Wolf, K.L., Pugh, H.G., Schroeder, L.S., Maier, M., Renfordt, R.E., Dacal, A., and Ortiz, M.E., Phys. Rev. Lett. 49, 1236 (1982).
40. Gale, C., Phys. Rev. C36, 2152 (1987).
41. Miller, J., Bercovitz, J., Claesson, G., Krebs, G., Roche, G., Schroeder, L.S., Benenson, W., van der Plicht, J., Winfield, J.S., Landaud, G., and Gilot, J.-F., Phys. Rev. Lett. 58, 2408 (1987) and Phys. Rev. Lett. 59, 519 (1987).
42. Miller, J., in Proc. of the 8th High Energy Heavy Ion Study, Lawrence Berkeley Report LBL-24580, p. 232 (1988), and private communications.
43. Benenson, W., Nucl. Phys. A495, 21c (1989).
44. VerWest, B.J., and Arndt, R.A., Phys. Rev. C25, 1979 (1982).

45. Lock, W.F., and Measday, D.F., "Intermediate Energy Nuclear Physics" (Methuen, London, 1970).
46. Bauer, W., Phys. Rev. C40, 715 (1989).
47. Noll, H., Grosse, E., Braun-Munzinger, P., Dabrowski, H., Heckwolf, H., Klepper, O., Michel, C., Müller, W.F.J., Stelzer, H., Brendel, C., and Rösch, W., Phys. Rev. Lett. 52, 1284 (1984).
48. Grosse, E., Nucl. Phys. A447, 611c (1985).
49. Bertsch, G.F., Phys. Rev. C15, 713 (1977).
50. Blann, M., Phys. Rev. Lett. 54, 2215 (1985); Phys. Rev. C32, 1231 (1985).
51. Aichelin, J., Phys. Lett. 164B, 261 (1985).
52. Cassing, W., Z. Phys. A329, 487 (1988).
53. Braun-Munzinger, P., and Stachel, J., Ann. Rev. Nucl. Part. Sci. 37, 97 (1987).
54. Vasak, D., Stöcker, H., Müller, B., and Greiner, W., Phys. Lett. 93B, 243 (1980).
55. Vasak, D., Greiner, W., Müller, B., Stahl, T., and Uhlig, M., Nucl. Phys. A428, 291c (1984).
56. Vasak, D., Greiner, W., Müller, B., J. Phys. G11, 1309 (1985).
57. Shyam, R., and Knoll, J., Phys. Lett. 136B, 221 (1984) and Nucl. Phys. A426, 606 (1984).
58. Bauer, W., Preprint MSUCL-734.
59. Csernai, L.P., and Kapusta, J.I., Phys. Rep. 131, 223 (1986).
60. Siemens, P.J., and Jensen, A.S., "Elements of Nuclei" (Addison Wesley, Redwood City, 1987).
61. Bauer, W., Phys. Rev. C 38, 1297 (1988).
62. Ornstein, L.S., and Zernicke, F., Proc. Sect. Sci. K. med. Akad. Wet. 17, 793 (1914).
63. Brown, G.E., and Siemens, P.J., unpublished.
64. Migdal, A.B., Zh. Eksp. Teor. Fiz. 61, 2209 (1971) and Soviet Phys., JETP 34, 1184 (1972).
65. Brown, G.E., and Weise, W., Phys. Rep. 27, 1 (1976).
66. Migdal, A.B., Rev. Mod. Phys. 50, 10 (1978).
67. Gyulassy, M., and Greiner, W., Ann. Phys. (N.Y.) 109, 485 (1977).
68. Ericson, T., and Weise, W., "Pions and Nuclei" (Clarendon, Oxford, 1988).
69. Suzuki, T., Fukuda, M., Ichihara, T., Inabe, N., Kubo, T., Nakagawa, T., Yoshida, K., Tanihata, I., Kobayashi, T., Suda, T., Shimoura, S., and Fujiwara, M., Phys. Lett. 257B, 27 (1991).
70. Niita, K., private communication.
71. Brockmann, R., Harris, J.W., Sandoval, A., Stock, R., Ströbele, H., Odyniec, G., Paugh, H.G., Schroeder, L.S., Renfordt, R.E., Schall, D., Bangert, D., Rauch, W., and Wolf, K.L., Phys. Rev. Lett. 53, 2012 (1984).

72. Odyniec, G., Bartke, J., Chase, S.I., Harris, J.W., Pugh, H.G., Rai, G., Rauch, G., Schroeder, L.S., Teitelbaum, L., Tincknell, M.L., Stock, R., Renfordt, R., Brockmann, R., Sandoval, A., Ströbele, H., Wolf, K.L., and Sullivan, J.P., in Proc. of the 8th High Energy Heavy Ion Study, Lawrence Berkeley Report LBL-24580, p. 215 (1988).
73. Chase, S.I., Barnes, P., Harris, J.W., Miller, J., Odyniec, G., Rauch, W., Teitelbaum, L., Tonse, S., Renfordt, R.E., and Tincknell, M.L., in: Proceedings of the Workshop on Nuclear Dynamics VI, Lawrence Berkeley Report LBL-28709, p.67 (1990).
74. Hahn, D., and Glendenning, N.K., Phys. Rev. C37, 1053 (1988).
75. Shuryak, E., Phys. Rev. D42, 1764 (1990).
76. Li, B.-A., and Bauer, W., Phys. Lett. 254B, 335 (1991).
77. Harris, J.W., NA35 collaboration, Nucl. Phys. A498, 133 (1989).
78. Schuhkraft, J., Helios collaboration, Nucl. Phys. A498, 79 (1989).
79. Atwater, T.W., Freier, P.S., and Kapusta, J.I., Phys. Lett. 199B, 30 (1987).
80. Lee, K.S., and Heinz, U., Z. Phys. C43, 425 (1989).
81. Kusnezov, D., and Bertsch, G.F., Phys. Rev. C40, 2075 (1989).
82. Brown, G.E., Stachel, J., and Welke, G.M., Phys. Lett. 253B, 19 (1991).
83. Chapters by Porile, N., *et al.*, Shuryak, E.V., Welke, G.M., in Ref. 1.
84. Danielewicz, P., and Odyniec, G., Phys. Lett. 157B, 146 (1985).
85. Keane, D., Beavis, D., Chu, S.Y., Fung, S.Y., Gorn, W., Liu, Y.M., VanDalen, G., Vient, M., in: Proceedings of the Workshop on Nuclear Dynamics IV, IU Report CONF-860270 UC-34C INC-40007-37, p. 151 (1986).
86. Danielewicz, P., Ströbele, H., Odyniec, G., Bangert, D., Bock, R., Brockmann, R., Harris, J.W., Pugh, H.G., Rauch, W., Renfordt, R.E., Sandoval, A., Schall, D., Schroeder, L.S., and Stock, R., Phys. Rev. C38, 120 (1988).
87. Gosset, J., Valette, O., Alard, J.P., Augerat, J., Babinet, R., Bastid, N., Brochard, F., De Marco, N., Dupieux, P., Fodor, Z., Fraysse, L., Gorodetzky, P., Lemaire, M.C., L'Hôte, D., Lucas, B., Marroncle, J., Montarou, G., Parizet, M.J., Poitou, J., Racca, C., Rahmani, A., Schimmerling, W., and Terrien, Y., Phys. Rev. Lett. 62, 1251 (1989).
88. Hartnack, C., Stöcker, H., and Greiner, W., in: Proceedings of the International Workshop on Gross Properties of Nuclei and Nuclear Excitation XVI, GSI report, p. 138 (1988).
89. Li, B.-A., Bauer, W., and Bertsch, G.F., Preprint MSUCL-777, to be published in Phys. Rev. C.